

Combinatorics of feedback in cellular uptake and metabolism of small molecules

Sandeep Krishna^{†‡}, Szabolcs Semsey[§], and Kim Sneppen[†]

[§]Department of Genetics, Eotvos Lorand University, Budapest H-1117, Hungary; and [†]Niels Bohr Institute, Blegdamsvej 17, 2100 Copenhagen, Denmark

Edited by H. Eugene Stanley, Boston University, Boston, MA, and approved November 5, 2007 (received for review July 3, 2007)

We analyze the connection between structure and function for regulatory motifs associated with cellular uptake and usage of small molecules. Based on the boolean logic of the feedback we suggest four classes: the *socialist*, *consumer*, *fashion*, and *collector* motifs. We find that the *socialist* motif is good for homeostasis of a useful but potentially poisonous molecule, whereas the *consumer* motif is optimal for nutrition molecules. Accordingly, examples of these motifs are found in, respectively, the iron homeostasis system in various organisms and in the uptake of sugar molecules in bacteria. The remaining two motifs have no obvious analogs in small molecule regulation, but we illustrate their behavior using analogies to fashion and obesity. These extreme motifs could inspire construction of synthetic systems that exhibit bistable, history-dependent states, and homeostasis of flux (rather than concentration).

homeostasis | network motif | regulation | sugar uptake

Feedback and biological regulation are two sides of the same coin, reflecting the need of the living cell to deal with changing environments, to generate cell to cell heterogeneity and to optimize cellular metabolism to a given external condition (1–6). The interplay between function and design of regulatory systems is a key issue in understanding cellular processes, and for engineering artificial biological circuits (7, 8). In a few relatively simple biological circuits, like the genetic switch in phage lambda (9), the connection between the regulatory logic and its biological function has been partially clarified. For larger scale regulatory networks, it has also been suggested that feed-forward motifs are associated with particular functions (10). However, feedback loops are, in fact, the most common network motifs in cellular organization, especially when one considers the regulation of small molecules (11), ranging from minerals to nutrients required for proper cellular function. A large class of cellular response systems are designed to regulate the flux and concentration of these molecules by controlling, via two feedback loops, the transport and metabolism pathways. Typically, these two loops are connected by a common transcriptional regulator that senses the concentration of the small molecule. In fact, almost half the transcription factors in *Escherichia coli* are directly regulated by a small molecule (12, 13).

Here we investigate the possible logical structures of such entangled loops involving small molecules and explicate, for these network motifs, a direct connection between structure and function of molecular regulation. There are four distinct logical structures for two entangled feedback loops, shown in Fig. 1. Inspired by their functional behavior we label the first two the *socialist* and the *consumer* motifs. The former balances the influx (transport) and outflux (metabolism) preventing large variations in the concentration of the small molecule. The latter, in contrast, responds by maximizing both influx and outflux.

The other two logical structures, the *fashion* and *collector* motifs, display a behavior that is somewhat pathological, quite common in human behavior but less common in cells. The *fashion* motif attempts to increase influx when the molecule is rare, but decreases it when the molecule is abundant, reminiscent of human response to fashionable goods which are valued for their scarcity. The *collector* motif displays bistability and the

ability to accumulate as much of the small molecule as it can, without consuming it: a seemingly senseless “Uncle Scrooge” strategy.

Four Combinations of Transport and Metabolic Feedback

Fig. 1 *Left* shows four possible combinations of entangled transport and metabolism feedback loops. In each case, the two feedback loops are connected by a transcriptional regulator (R) that senses the concentration of a particular small molecule (s). One loop regulates transcription of the transport proteins (T) facilitating the influx of the small molecule, while the other controls transcription of enzymes (E) responsible for the metabolism of s (see Fig. 2 for an illustration of the processes occurring in the cell for one of the motifs). In the scenario we consider, the number of regulators is typically smaller than the level of s , which in turn, is much smaller than the flux.[¶]

Each loop can be characterized by a sign that denotes that the loop implements a positive (+) or negative (–) feedback.^{||} In describing the logic of the entangled loop motifs, we use the notation of two signs, e.g., (+ –), which means that the transport loop is positive and the metabolism loop negative. Thus, there are four logical structures: the *socialist* (– –), the *consumer* (+ –), the *fashion* (– +), and the *collector* (+ +). Each can, in turn, be implemented in two distinct but logically equivalent ways, depending on whether s inhibits or activates R . This we denote using the notation (+ – i) or (+ – a), where the i (respectively, a) indicates inhibition (activation) of R by s . In Fig. 1, we show only the a motifs, but our conclusions hold for the i motifs also [as shown in supporting information (SI) *Text*].

Results and Discussion

Functional Behavior of the Four Motifs. The plots in Fig. 1 show the steady state behavior of s and the influx σT as a function of σ , which is a measure of the amount of extracellular s . The plots are produced by solving the differential equations describing the temporal dynamics of s , E and T (see *Materials and Methods*). The black line in each plot shows the “standard” case where the two loops are equally strong.

The (– –) motif, with maximal negative feedback is the only one where the steady state s level increases slower than linearly

Author contributions: S.K., S.S., and K.S. designed research; S.K., S.S., and K.S. performed research; S.K., S.S., and K.S. contributed new reagents/analytic tools; S.K., S.S., and K.S. analyzed data; and S.K., S.S., and K.S. wrote the paper.

The authors declare no conflict of interest.

This article is a PNAS Direct Submission.

†To whom correspondence should be addressed. E-mail: sandeep@nbi.dk.

[¶]For iron regulation in *E. coli*, we estimate a γ of ≈ 100 (14) (γ is the rate of consumption of the small molecule by one unit of metabolic enzyme). For nutritional molecules like galactose and lactose (15), the estimate is much higher. We use $\gamma = 100$, but increasing it does not change any of our conclusions.

^{||}Note that a positive metabolism loop does *not* mean an increase of the metabolic rate with increase of s . Rather, it means exactly the opposite: an increase of s leads to a decrease of the metabolic rate, hence there is a *positive* feedback of the s level onto itself.

This article contains supporting information online at www.pnas.org/cgi/content/full/0706231105/DC1.

© 2007 by The National Academy of Sciences of the USA

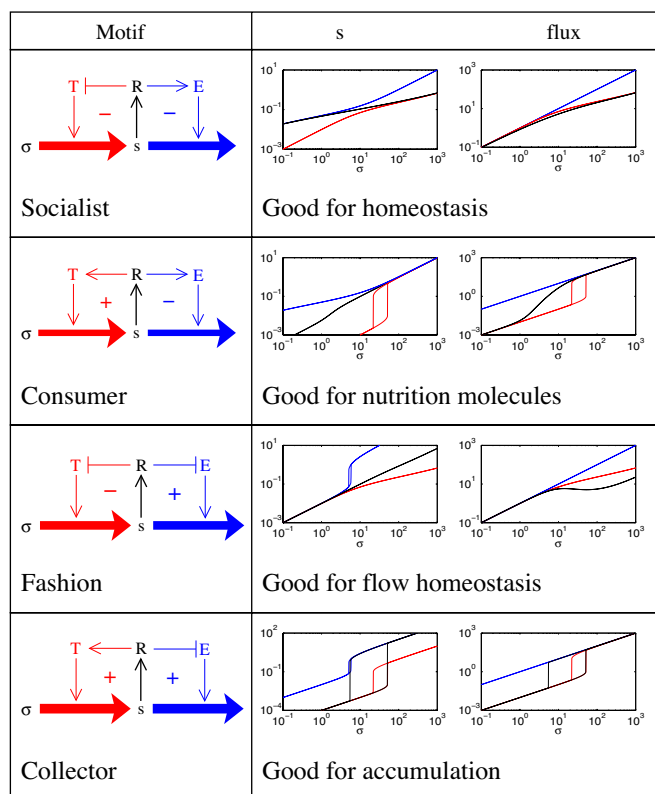


Fig. 1. Behavior of four entangled feedback loop motifs. Plots show the steady state values of s (middle column) and influx ($\sigma T = \gamma E s + s$, Right) as a function of σ . In all plots, the black curve shows the behavior for standard parameter values (see *Materials and Methods*). The red curve shows the behavior when only the transport loop is active, i.e., $E = 1$. The blue curve is produced by keeping $T = 1$, i.e., only the metabolism loop is active. The plots were made by two sweeps of the value of σ , the first from 0.1 to 1,000, and the second from 1,000 back to 0.1. At each σ value, we start E , T , and s concentrations at the previous steady-state values, and then integrate the equations until a new steady state is reached. Thus, for each σ , the plots contain information from two simulations, one starting from a lower value of s , the other from a higher. For systems where there is no bistability, the s and flux vs. σ curves for the two sweeps are identical. However, where there is some bistability, the two curves differ, i.e., they show hysteresis.

with σ . Thus, this motif keeps s relatively insensitive to changes in extracellular conditions.

The $(+ -)$ motif shows a linear dependence of s on σ . The influx however can increase and decrease faster than linearly as σ is changed, due to the positive feedback in the T loop. The result is a rapid opening of both the transport and consumption channels as soon as the small molecule is detected extracellularly. Thus the function of the $(+ -)$ motif is to maximize both the influx and outflux of s .

The most striking feature of the $(- +)$ motif is that the flux increases linearly at small σ but then decreases at higher σ values, and subsequently again increases at even higher σ . This motif therefore has a broad range of σ values where the flux does not increase, whereas the amount of intracellular s increases substantially.

The $(+ +)$ motif produces robust bistability, as illustrated by the hysteric behavior. The large s branch of the hysteric curves have the characteristic that $E \approx 0$ and therefore the level of s is about as large as the total flux. Thus, this motif is the one, among all of the entangled loop motifs, that can give the highest concentration of intracellular s .

These steady-state properties capture the main functional behavior of the four motifs. Their dynamical response to per-

turbations in the external small molecule concentration, examined in the supplementary material, can also be inferred from the steady-state behavior. Essentially, even for moderate-sized perturbations, the new steady state is reached in around one unit of time, and the motifs respond faster when the steady-state level of E is higher (see *SI Fig. 5*). A linear stability analysis reconfirms this overall fast response, except the slowing down close to the onset of bistability in the collector motif (see *SI Fig. 4*).

In the subsequent sections, we discuss the relevance of the motifs in various contexts.

The Socialist Motif. We call the $(- -)$ motif the *socialist* because at low levels of extracellular s (low σ) it increases transport and reduces the metabolism, whereas at high levels of extracellular s , it does the opposite. Thus, the two negative feedback loops help maintain s robustly within a small concentration range. Such behavior would be ideal for a system responsible for maintaining homeostasis. And indeed, a regulatory system with this logic is found in the iron homeostasis system in mammals (16): iron activates the Ferric uptake regulator (Fur), which represses transcription initiation of iron uptake genes, and enhances production of iron-using proteins. For most organisms, iron is essential for several proteins, but is poisonous at high concentrations. There, the $(- -)$ motif maintains the loosely bound iron within a narrow concentration range, and at the same time allows a high consumption of iron molecules by certain proteins that bind iron strongly.

The Consumer Motif. The $(+ -)$ motif we term the *consumer*, because any amount of extracellular small molecule results in the increase of both transport and metabolism. Thus, it is ideal for food molecules. This logic is, in fact, typical for sugar transport and metabolism in prokaryotes. The *gal* (17) and *lac* (18, 15) operons in *E. coli* are the most well studied of such systems. They both use the sugar molecule to inhibit the transcription factor regulating transport and metabolism, the $(+ - i)$ motif. In contrast, maltose (19) and arabinose (20) work by activating the regulation of transport and metabolism, the $(+ - a)$ motif. In the natural systems, transport and metabolic genes can be part of a single operon ($K_E = K_T$), as in *lac* (18), or separate operons, as in *gal* (17). The latter arrangement allows noncoordinated regulation of transport and metabolism and therefore can be engineered to become bistable. This was also demonstrated by experiments on modified lactose and arabinose systems (6, 21), where the accompanying negative feedback loop was eliminated by inactivating E or using a nonmetabolizable analogue of s , in agreement with our predictions from a similar cutting of the metabolic loop in Fig. 1. Another *consumer* system is associated with the uptake and processing of the quorum sensing molecule AI-2 in *E. coli* (22), a context where the maximization of the influx prevents accumulation of external AI-2 and, hence, oversaturation of the quorum sensing abilities of the population.

The Fashion Motif. As the motif $(- +)$ is indeed the opposite of the *consumer* motif, both logically and functionally, it is not surprising that we have not found any simple example of it in the regulation of small molecules in living cells. However, its behavior (and the reason we call it the *fashion* motif) can be illustrated in terms of a market model for a product which is desirable in small amounts. In such a scenario, the resource, s , is analogous to a fashion product, E to the consumers, and T to the producers. R can be considered the value of the product, measured in terms of how much people desire it. When there is plenty of the product s in the market, its value R decreases, which in turn decreases its consumption (a positive metabolism feedback loop) as well as the desire amongst producers to make more of it (a negative transport feedback loop), making it a $(- +)$ motif. The nonmonotonicity of the flux of the *fashion* motif

| Motif | s | flux |
|-------|--|--|
| | At low σ , s grows linearly with σ At high σ prevents s from growing large | At low σ , flux grows linearly with σ At high σ prevents flux from growing large |
| | Causes bistability Outside the bistable range s is proportional to σ | Causes bistability Outside the bistable range flux is proportional to σ |
| | At high σ , s grows linearly with σ At low σ prevents s from falling too low | Flux grows linearly with σ for all values of σ |
| | Causes bistability Outside the bistable range s is proportional to σ | Flux grows linearly with σ for all values of σ |
| | s is kept within a narrow range at both low and high σ | At low σ , flux grows linearly with σ At high σ prevents flux from growing large |
| | No bistability s grows (almost) linearly with σ | No bistability flux has steep increase at intermediate σ |
| | No bistability s grows linearly with σ | flux is non-monotonic for intermediate σ outside this range it grows linearly with σ |
| | Bistability; s is proportional to σ Bistable range is larger than either single loop | Bistability; flux is proportional to σ Bistable range is larger than either single loop |

Fig. 3. The main features of single and double loops. The figure lists first all four single loop motifs, followed by the four two-loop motifs of Fig. 1, along with the main characteristics of their steady state behavior. Those features of the two-loop motifs that are significantly different from a simple sum of the single loop behaviors are highlighted in yellow.

Steady-State Behavior of Single Feedback Loops. The qualitative features of two-loop motifs are robust to a weakening of one or the other loop (see *SI Text*). However, when one loop is weakened so much that the motif is reduced to essentially a single loop the behavior can be quite different. To quantify this, we removed one of the feedback loops in each of the motifs, cutting the link between R and either T or E , by fixing $T = 1$ or $E = 1$. Thus $(1 -)$ means that we set $T = 1$ while keeping regulation of E identical to its regulation in the full motif, which for example may be $(- -)$. For each motif in Fig. 1, the blue curve shows the behavior for the constant T case (i.e., only the metabolic loop operates), whereas the red curve shows the behavior for the constant E case (only the transport loop operates). In general, a negative E loop $(1 -)$ is capable of constraining s levels at low σ , whereas a negative T loop $(- 1)$ constrains s at high σ . A positive T loop $(+ 1)$ produces bistability in s and the flux. A positive E loop $(1 +)$, on the other hand, produces a weaker bistability only in s .

Two-Loop Motifs Are More than the Sum of their Single Loops. In Fig. 3, we summarize the main behavioural features of two-loop

motifs and their constituent single loops. The near constant value of s in $(- -)$ comes from the $(1 -)$ ability to constrain s for low σ , and the $(- 1)$ ability to constrain s at high σ . Thus the functionality of $(- -)$ is dominated by the submotif that best prevents large variation of s and flux. The $(+ -)$ obtains a steady increase in s and a step like increase in flux with σ by using the $(1 -)$ motif's ability to "smooth out" the bistability associated to the $(+ 1)$ motif. The $(- +)$ motif exhibits a remarkable nonmonotonic behavior of flux, which cannot be obtained from any of the submotifs. The $(+ +)$ motif maximizes bistability, by extending it to the extreme of the two bistable regions of its submotifs. The width of this large bistable region mostly depends on K_T , whereas the enzyme regulation K_E affects its position (see *SI Text*). Overall, we find that whole two-loop motifs are more than a simple sum of their parts.

Self-Regulation. In the regulation of several sugars, such as lactose (29), galactose (30), and arabinose (20), the main regulator is known to regulate its own activity in addition to transport and metabolism. This action of R on itself is the simplest addition to our two-loop motifs. In supplementary material we explore the effects of such self-regulation for each of the motifs. The main effect of self-activation of R is to enhance the tendency to produce bistable behavior of fluxes, whereas self-repression reduces the signaling from s across the regulator R .

Going Beyond Two Loops. Our analysis of two entangled feedback loops creates a framework for analyzing small molecule regulatory circuits composed of multiple entangled feedback loops. For instance, the regulation of iron in *E. coli*, although being dominated by interactions that form a *socialist* motif (14, 31), also contains a positive feedback on the metabolism side involving usage of iron in FeS clusters (32). Preliminary investigation (data not shown) suggests that two metabolism loops, connected like this in "parallel" (as opposed to the "series" connection between a transport and metabolism loop), are additive in behavior. Due to this additiveness, iron regulation in *E. coli* is able to minimize variation of both the concentration of iron (a property of the *socialist* part) as well as the flux (a property of the *fashion* part) (14). It remains for future work to examine design principles for combinations of parallel and serially connected feedback loops.

Materials and Methods

In all of the motifs of Fig. 1 we track the concentrations E , T , and s . The dynamics of s is given by

$$\frac{ds}{dt} = \sigma T - \gamma E s - s. \quad [1]$$

The first term models the transport rate. The rate of transport of s per T protein, σ , is a measure of extracellular s . The next term models the metabolism of s by the E proteins, with γ parametrizing the speed of the consumption. The last term represents dilution of s due to cell growth. We have chosen the units of time to be one cell generation, and will assume this is much smaller than the metabolic consumption rate per E protein.

We assume that R and s interact by forming a complex, and that this complex is in equilibrium at all times.^{††} Then the concentrations of free and bound R are

^{††}In the Lac system, the association and dissociation of the lactose–LacI complex have been measured to be occurring on a time scale faster than a second (33, 34), which is much faster than transcription, translation and degradation processes. In the iron system, the Fe–Fur complex has a $K_D \approx 20 \mu\text{M}$ (14). Association and dissociation rates have not been separately measured, but assuming that association is diffusion limited, we would get a dissociation time scale of milliseconds, which is also much faster than other processes. Therefore, we believe the assumption of equilibrium is reasonable.

$$R_{\text{free}} = R^{\text{tot}} \frac{1}{1 + (s/K)^{h_s}}; \{R_s\} = R^{\text{tot}} \frac{(s/K)^{h_s}}{1 + (s/K)^{h_s}}, \quad [2]$$

where R^{tot} is total R , assumed to be much smaller than s , K sets the binding strength of the $\{R_s\}$ complex, with h_s being a Hill coefficient.

The concentration of the active form of R , denoted R^* , is either R_{free} or $\{R_s\}$ depending on the motif. The dynamics of E is then given by:

$$\frac{dE}{dt} = A_E(R^{\text{tot}}, s) - E; A_E = \frac{A_{\text{max}}}{1 + (R^*/K_E)^{\pm h_E}} + \varepsilon, \quad [3]$$

where we use $+h_E$ if R represses E and $-h_E$ if it activates. The “leak” ε represents a small basal level of activity. A similar equation is written for T . $K_{E,T}$

and $h_{E,T}$ are the relevant dissociation constants and Hill coefficients. Equations 1–3 can describe all four motifs shown in Fig. 1. Default parameters are: $h_s = 1$, $K = 1$, $h_E = 2$, $K_E = 1$, $h_T = 2$, $K_T = 1$, $\gamma = 100$, $R^{\text{tot}} = 10$, $A_{\text{max}} \approx 1$, $\varepsilon = 0.01$. For more details, see *SI Text*. To obtain trajectories, the differential equations were numerically integrated using a Runge–Kutta algorithm with adaptive step sizes. Steady states can be obtained by either running the integrator for long times, or by solving the algebraic problem produced by setting all derivatives to zero in the above equations.

ACKNOWLEDGMENTS. This work was funded by the Danish National Research Foundation through the Center for Models of Life, and by a Marie Curie International Reintegration Grant within the 6th European Community Framework Program. S.S. is grateful for the Janos Kolyai Research Fellowship of the Hungarian Academy of Sciences.

1. Thomas R, D’Ari R (1990) *Biological Feedback* (CRC Press, Boca Raton, FL)
2. Bhalla US, Iyengar R (1999) *Science* 283:381–387.
3. Ferrell JE, Jr (2002) *Curr Opin Cell Biol* 14:140–148.
4. Angeli D, Ferrell JE, Jr, Sontag ED (2004) *Proc Natl Acad Sci USA* 101:1822–1827.
5. Thattai M, van Oudenaarden A (2004) *Genetics* 167:523–530.
6. Smits WK, Kuipers OP, Veening JW (2006) *Nat Rev Microbiol* 4:259–271.
7. Elowitz MB, Leibler S (2000) *Nature* 403:335–338.
8. Gardner TS, Cantor CR, Collins JJ (2000) *Nature* 403:339–342.
9. Oppenheim AB, Kobilier O, Stavans J, Court DL, Adhya S (2005) *Annu Rev Genet* 39:409–429.
10. Mangan S, Alon U (2003) *Proc Natl Acad Sci USA* 100:11980–11985.
11. Krishna S, Andersson AMC, Semsey S, Sneppen K (2006) *Nucleic Acids Res* 34:2455–2462.
12. Anantharaman V, Koonin EV, Aravind L (2001) *J Mol Biol* 307:1271–1292.
13. Babu MM, Teichmann SA (2003) *Nucleic Acids Res* 31:1234–1244.
14. Semsey S, Andersson AMC, Krishna S, Jensen MH, Massé E, and Sneppen K (2006) *Nucleic Acids Res* 34:4960–4967.
15. Wong P, Gladney S, Keasling JD (1997) *Biotechnol Prog* 13:132–143.
16. Massé E, Arguin M (2005) *Trends Biochem Sci* 30:462–468.
17. Weickert MJ, Adhya S (1993) *Mol Microbiol* 10:245–251.
18. Jacob F, Monod J (1961) *J Mol Biol* 3:318–356.
19. Richet E, Raibaud O (1989) *EMBO J* 8:981–987.
20. Schleif R (2000) *Trends Genet* 16:559–565.
21. Ozbudak EM, Thattai M, Lim HN, Shraiman BI, van Oudenaarden A (2004) *Nature* 427:737–740.
22. Xavier KB, Bassler BL (2005) *J Bacteriol* 187:238–248.
23. Donangelo R, Sneppen K (2002) *Physica A* 316:581–591.
24. Lamark T, Rokenes TP, McDougall J, Strom AR (1996) *J Bacteriol* 178:1655–1662.
25. Rokenes TP, Lamark T, Strom AR (1996) *J Bacteriol* 178:1663–1670.
26. Ansari AZ, Bradner JE, O’Halloran TV (1995) *Nature* 374:370–375.
27. Yanofsky C, Crawford IP (1987) in *Escherichia coli and Salmonella thyphymurium: Cellular and Molecular Biology*, eds Neidhart FC, Curtiss R, Ingraham JL, Lin ECC, Low KB, Magasanik B, Reznikoff WS, Riley M, Schaechter M, Umberger HE (Am Soc Microbiol Press, Washington, DC), Vol 2, pp 1454–1472.
28. Snell EE (1975) *Adv Enzymol* 42:287–333.
29. Abo T, Inada T, Ogawa K, Aiba H (2000) *EMBO J* 19:3762–3769.
30. Semsey S, Krishna S, Sneppen K, Adhya S (2007) *Mol Microbiol* 65:465–476.
31. Mitarai N, Andersson AMC, Krishna S, Semsey S, Sneppen K (2007) *Phys Biol* 4:164–171.
32. Outten FW, Djaman O, Storz G (2004) *Mol Microbiol* 52:861–872.
33. Friedman BE, Olson JS, Matthews KS (1976) *J Biol Chem* 251:1171–1174.
34. Dunaway M, Olson JS, Rosenberg JM, Kallai OB, Dickerson RE, Matthews KS (1980) *J Biol Chem* 255:10115–10119.